Geophysical Research Letters

RESEARCH LETTER
10.1029/2019GL086133

Key Points:
- A robust positive trend in MJO Phase 4-6 days during 1979-2015 winters based on the Wheeler-Hendon RMM index could be exaggerated
- Cautions need to be exercised when applying the RMM index for studies on the low-frequency variability of MJO activity

Supporting Information:
- Supporting Information

Correspondence to:
X. Jiang,
xianan@ucla.edu

Citation:
Lyu, M., Jiang, X., & Wu, Z. (2019). A cautionary note on the long-term trend in activity of the Madden-Julian Oscillation during the past decades. *Geophysical Research Letters*, *46*. https://doi.org/10.1029/2019GL086133

Received 5 NOV 2019
Accepted 26 NOV 2019
Accepted article online 3 DEC 2019

A Cautionary Note on the Long-term Trend in Activity of the Madden-Julian Oscillation During the Past Decades

Mengxia Lyu[1,2], Xianan Jiang[2,3], and Zhiwei Wu[4]

[1]College of Atmosphere Sciences, Nanjing University of Information Science and Technology, Nanjing, China, [2]Joint Institute for Regional Earth System Science and Engineering, University of California, Los Angeles, CA, USA, [3]Jet Propulsion Laboratory, California Institute of Technology, Pasadena, CA, USA, [4]Department of Atmospheric and Oceanic Sciences/Institute of Atmospheric Sciences, Fudan University, Shanghai, China

Abstract Recent studies suggest that frequency of active phases of the Madden-Julian Oscillation (MJO) over the Maritime Continent and western Pacific, that is, the MJO Phases 4–6 defined by the real-time multivariate MJO (RMM) index, has increased in recent winters. A robust positive trend in MJO Phase 4–6 days during 1979–2015 winters is confirmed in this study. Our analyses, however, suggest that this trend could be exaggerated due to the blended low-frequency variability signals in the RMM. When the winter RMM is reconstructed using anomalous fields after removing their winter mean instead of the previous 120-day mean as for the original RMM, the robust trend in MJO Phase 4–6 days can no longer be detected. Therefore, cautions need to be exercised when applying the RMM for studies on the low-frequency variability and climate trend in MJO activity and using the derived MJO variability to interpret associated changes in climate systems.

Introduction

Since the discovery of the Madden-Julian Oscillation (MJO) in 1970s (Madden & Julian, 1971), the critical role of the MJO in the Earth's hydrological cycle has been fully recognized (Lau & Waliser, 2012; Zhang, 2005). Despite its tropical origin, the MJO exerts tremendous influences on global climate and weather (e.g., Zhang, 2013). Due to its intermediate period of 30–60 days, the MJO has been considered one of the primary subseasonal predictability sources beyond the deterministic weather forecasts (e.g., Gottschalck et al., 2010; Vitart et al., 2012; Waliser, 2012). The continuous improvement of MJO prediction skill in the recent decades has promoted great enthusiasm in the community in exploring potentials for the extended range prediction of extreme weather activities (e.g., Baggett et al., 2018; Jiang et al., 2018; Lee et al., 2018; Lin, 2018; Mundhenk et al., 2018; Vitart & Robertson, 2018; Wang et al., 2018; Xiang et al., 2015; Xiang et al., 2019).

To better understand and predict the low-frequency changes in activity of weather extremes, great efforts have been devoted to understanding changes of MJO activity during the past decades and in a future climate. Both observational (Lee & Seo, 2011; Slingo et al., 1999) and modelling studies (e.g., Adames et al., 2017; Arnold et al., 2015; Chang et al., 2015; Liu et al., 2013; Maloney et al., 2019) suggest that the MJO precipitation variations tend to enhance in a warming climate, along with weak increase or even decrease of MJO wind variability and teleconnections due to increase of tropical static stability (Bui & Maloney, 2018; Maloney et al., 2019; Wolding et al., 2017). Meanwhile, an increase of frequency of occurrence of active MJO events is also suggested under a warming scenario (Jones & Carvalho, 2006; Jones & Carvalho, 2011; Song & Seo, 2016).

In particular, a recent observational study by Yoo et al. (2011) illustrates that the frequency of a particular MJO phase with enhanced convection over the Maritime Continent (MC) and western Pacific (WP), that is, the MJO Phases 4–6 as defined by the real-time multivariate MJO (RMM) index (Wheeler & Hendon, 2004; hereafter WH04), has significantly increased in boreal winter during recent decades. This decadal change in MJO activity is further linked to variations in the lower-tropospheric moist static energy pattern associated with the Pacific Decadal Oscillation (Xiu et al., 2019). The latent heat release associated with MJO convection over the MC and WP can effectively trigger the planetary-scale Rossby waves (e.g., Hoskins & Karoly, 1981; Stan et al., 2017), resembling a positive phase of the Pacific North America teleconnection pattern (Wallace & Gutzler, 1981), and can induce warm surface air temperature anomalies over a large portion of the Arctic (e.g., Lee et al., 2011; Yoo et al., 2011). The increased frequency of active MJO phases over the MC and WP in the recent decades, therefore, could promote more frequent occurrence of positive Pacific North America patterns and thus lead to Arctic warming (Lee et al., 2011; Seo et al., 2016; Yoo et al., 2011; Yoo et al., 2012), featuring a so-called tropically excited Arctic warming mechanism to interpret the recent Arctic amplification (e.g., Lee, 2014).

In this study, however, we demonstrate that this robust increasing trend in days of the MJO Phases 4–6 during the past decades could be largely exaggerated by using the WH04 RMM index. Therefore, cautions need to be excised when using this trend for interpreting associated low-frequency variability in the global climate system. In the following discussions, the term “low-frequency variability” is used to represent climate variability from the interannual to decadal time scales, as well as the long-term climate trend.

Data and Methods

The RMM index by WH04 from 1979 to 2016 can be obtained from the Australian Bureau of Meteorology (http://www.bom.gov.au/climate/mjo/). These two daily RMM coefficients, RMM_1 and RMM_2, are derived as the principal components of the two leading empirical orthogonal function (EOF) of combined equatorially (15°S–15°N) averaged anomalous fields of zonal winds at 200 (u200) and 850 hPa (u850) and the outgoing longwave radiation (OLR). Before conducting the EOF analysis, the climatological seasonal cycle (annual mean and first three annual harmonics) is first removed from each variable. Then, the interannual variability associated with ENSO, derived by a linear regression to an ENSO index, is removed. Finally, a mean of the previous 120 days is further subtracted to remove the long-term variability. Daily MJO amplitude and phase can then be derived based on the two RMMs.

A series of MJO indices are constructed to test the robustness of the original RMM. Daily u200 and u850 data from the NCEP-NCAR reanalysis (Kalnay et al., 1996) and the NOAA OLR (Liebmann & Smith, 1996) from 1979 to 2016 are also used. Following WH04, daily anomalies of these variables are obtained by removing the climatological seasonal cycle for the period of 1979–2016 and then their mean values during the previous 120 days. Note that the removal of signals associated with ENSO is skipped here, as previously found to have minor effects (Gottschalck et al., 2010; Lin et al., 2008). Daily reconstructed RMM_1 and RMM_2 can then be obtained by projecting the combined anomalies of these three variables onto the two precomputed combined EOF patterns from WH04 (Vitart, 2017). As to be shown below, the reconstructed RMMs following the above approach (hereafter the CTRL experiment) well duplicate the original RMMs. Four sensitivity experiments are further conducted to examine how the detailed approaches for deriving the daily RMMs can affect the detected long-term include

1. *Exp_no_120day*. Same as CTRL, except that mean values from previous 120 days are not removed when calculating daily anomalies of OLR, u850, and u200;
2. *Exp_winter_mean*. Same as CTRL, except that the corresponding winter (November–April) mean, instead of the previous 120-day mean, is removed to get daily winter anomalies;
3. *Exp_120day_centered*. Same as CTRL, except that the mean of 60 days before and 60 days after, instead of previous 120 days, is removed from daily anomalies;
4. *Exp_20_120d_filter*. anomalies associated with the MJO are extracted by the 20- to 120-day Lanczos bandpass filtering (Duchon, 1979) after removal of the climatological seasonal cycle, rather than by subtracting the previous 120-day mean as in CTRL.

Results

Following Yoo et al. (2011), days of each MJO phase during winters (November–April) from 1979 to 2015 are calculated by the total number of days of the particular MJO phase when the MJO amplitude, defined by $\sqrt{RMM_1^2 + RMM_2^2}$, is greater than 1. Figure 1a illustrates occurrence frequency of each MJO phase during winters of 1979–1988 and 2006–2015 based on the WH04 RMM index. A notable increase (decrease) in frequency of the MJO Phases 4–6 (1–2) in the recent winters, as reported by Yoo et al. (2011), is clearly evident although strong year-to-year variability is noted by the error bars. A significant positive trend in the MJO Phase 4–6 days during the 36 winters is further clearly illustrated in Figure 1b, which again suggests more frequent occurrence of active phases of the MJO over the MC and WP in recent decades, and tends to

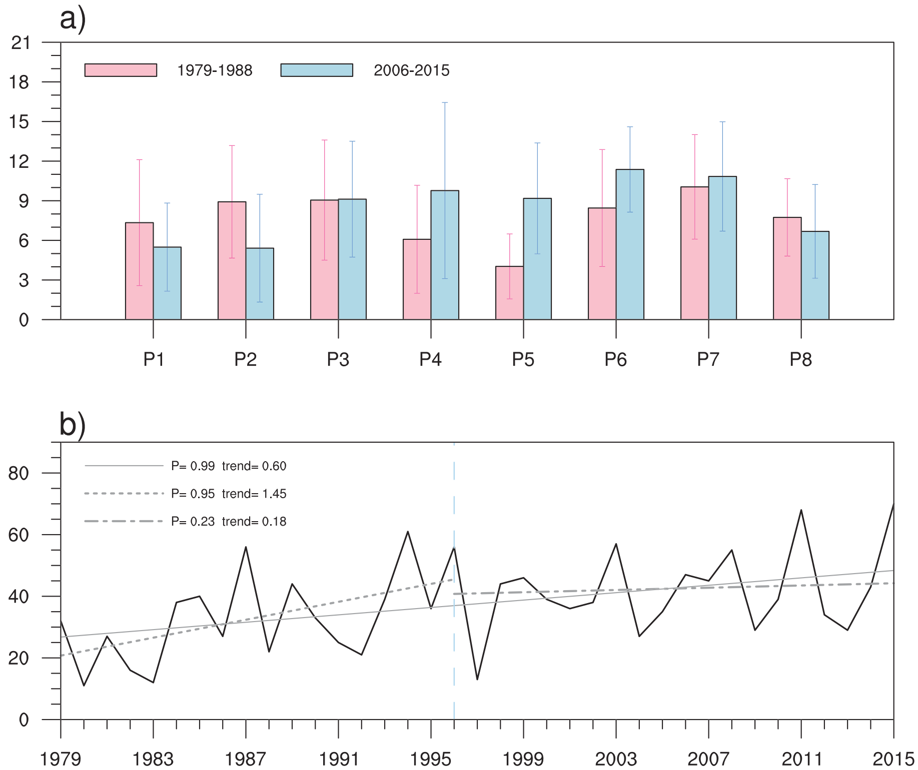

Figure 1. (a) Frequency of each MJO phase during the winters of 1979–1988 (pink) and 2006–2015 (blue); (b) days of MJO Phases 4–6 during each winter for the period of 1979–2015. The grey lines in (b) represent linear trends during the entire or a part of the 36-year period with their corresponding trend (units: days yr^{-1}) and statistical significance p value shown in the legend. All results are based on the original WH04 RMM MJO index.

support the aforementioned tropically excited Arctic warming mechanism hypothesis in interpreting the recent Arctic amplification. Further detailed examination in Figure 1b indicates that the strongest positive trend is observed during the period of 1979–1996, while the trend from 1997 to 2015 is relatively weak and statistically insignificant. Note that this robust positive trend in MJO activity is not sensitive to the threshold in defining strong MJO (supporting information Figure S1).

Table 1
Correlation of the Reconstructed Daily MJO Indices With the Original WH04 RMM_1 and RMM_2 and Year-to-Year MJO Phase 4–6 days During Winters From 1979 to 2015 Between Those Based on WH04 and Reconstructed RMM Indices

	Correlations with WH04				
Experiments	Daily PC_1	Daily PC_2	Phase 4–6 days in 36 winters	Trend (days/yr)	*P*_value
Ctrl	0.95	0.96	0.91	0.67	0.99
Ctrl_olr	0.74	0.73	0.59	0.16	0.62
Ctrl_u850	0.88	0.84	0.83	0.73	0.99
Ctrl_u200	0.85	0.84	0.82	0.43	0.95
Exp_no_120day	0.82	0.83	0.59	0.41	0.81
Exp_winter_mean	0.82	0.86	0.53	0.16	0.66
Exp_20_120d_filter	0.87	0.88	0.66	0.24	0.84

Note. Long-term linear trend (with red numbers being statistically significant at 95% level) and significance test *P* values of the MJO phases 4–6 days during the 36 winters are also illustrated. Significance test are based on the Mann-Kendall (M-K) approach.

To better understand the positive trend in frequency of occurrence of the MJO Phases 4–6 in the recent decades, days of the MJO Phase 4–6 for each winter during 1979–2016 period are also calculated based on the reconstructed RMMs (the CTRL experiment). Daily RMMs reconstructed from the combined OLR, u850, and u200 anomalies are highly correlated to the original RMMs during the 36 winters, with correlations of 0.95 and 0.96 for RMM_1 and RMM_2, respectively (Table 1). Meanwhile, the year-to-year variations in the MJO Phase 4–6 days in CTRL (black curve in Figure 2) also exhibit a very high correlation (0.91) with that based on the original RMM index, with a similar significant trend of 0.67 day yr^{-1}. Therefore, the reconstructed RMMs in CTRL well reproduce the original RMMs.

Daily reconstructed indices using OLR, u850, and u200 only based on CTRL (hereafter CTRL_olr, CTRL_u850, and CTRL_u200) can also be derived by projecting anomalies of these individual fields onto their corresponding patterns in the two combined EOFs precalculated by WH04. Correlations between the daily indices of individual variables and the original RMMs can indicate the relative role of these

10.1029/2019GL086133

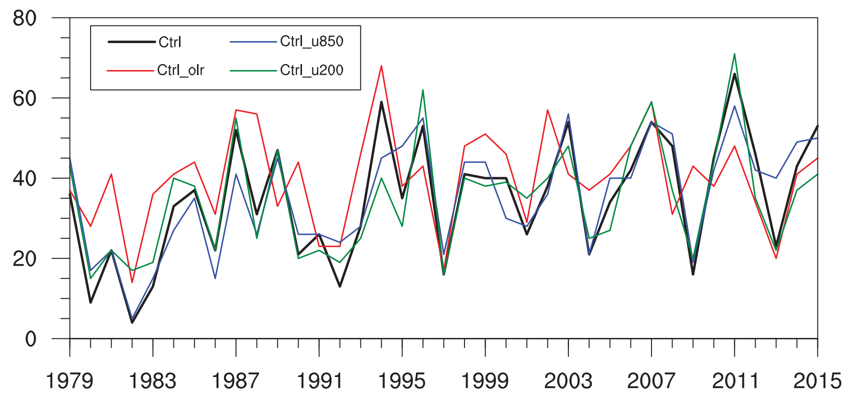

Figure 2. Days of the MJO Phases 4–6 in each winter from 1979 to 2015 based on the reconstructed RMM index (i.e., the CTRL experiment) along with days defined by the leading two PCs based on individual valuables of the OLR (red), u850 (blue), and u200 (green). See text for more details.

variables in contributing to the combined RMM index. As shown in Table 1, correlations between the daily indices based on the OLR only (CTRL_olr) and the original RMMs are much lower than those for u850 and u200, suggesting a more dominant role of circulation anomalies for the RMM index as previously reported (Kiladis et al., 2013; Straub, 2013). Meanwhile, the year-to-year variations in the MJO Phase 4–6 days can also be similarly calculated using the two daily coefficients based on OLR, u850, and u200, respectively, and are shown by color curves in Figure 2. Significant positive trends are discerned in the u850 and u200 indices but not in OLR (Table 1). Also, higher correlations between the MJO Phase 4–6 days based on u850 and u200 against that by the original RMM index are noted in Table 1. Therefore, the positive trend in the MJO Phase 4–6 days based on the original RMMs could be mainly attributed to variations in u200 and u850 rather than the OLR. Note that a lack of significant trends in MJO phase 4–6 days is also found by using an OLR-based MJO index (Kiladis et al., 2013) (supporting information Figure S2).

Since the reconstructed RMMs in CTRL can well reproduce the original RMMs, particularly the increasing trend in the MJO Phase 4–6 days, we next explore how sensitive this trend is to the detailed techniques used for deriving the RMM index in the four aforementioned sensitivity experiments. In the first experiment (Exp_no_120day), since the mean values from previous 120 days are not removed when calculating anomalies of OLR, u850, and u200, low-frequency signals are retained and projected onto the MJO EOFs. The correlations between the daily MJO index from Exp_no_120day and the original RMMs are significantly reduced compared to that from CTRL (Table 1), suggesting that removal of the previous 120-day mean significantly impacts on the calculated MJO index. As expected, days for the MJO Phases 4–6 during the 36 winters based on Exp_no_120day (Figure 3a) exhibit strong interannual variability associated with ENSO. Several winters with the minimum MJO Phase 4–6 days are associated with El Nino, for example, 1982/1983, 1997/1998, 2009/2010, and 2015/2016 winters, while several winters with the maximum peaks in MJO Phase 4–6 days are linked to La Niña, for example, 1998/1999, 2007/2008, and 2011/2012. The more (less) MJO Phase 4-6 days during La Niña (El Niño) winters are due to projection of OLR and u-wind anomalies corresponding to enhanced (suppressed) convection near the MC onto the MJO index. Interestingly, while a positive trend in the MJO Phase 4–6 days is still evident in Exp_no_120day, it is much weaker than that in CTRL and becomes statistically insignificant.

In Exp_winter_mean, where the low-frequency variability is removed by subtracting the corresponding winter (November–April) mean rather than the previous 120-day mean in CTRL, the robust trend in the MJO Phase 4–6 days as seen in CTRL can no longer be detected (Figure 3b); meanwhile, its year-to-year variability becomes rather weaker than that in CTRL, suggesting that the strong interannual variability in MJO activity in CTRL and the original RMMs is largely due to projection of the long-term variability signals. Additionally, results from the Exp_20_120d_filter experiment, in which anomalies associated with the MJO are extracted using an intraseasonal bandpass filtering, also suggest a rather weak and insignificant trend in MJO activity. While the u-wind from the NCEP-NCAR reanalysis is used for reconstruction of RMM indices in CTRL and other experiments, very similar results can be obtained if using u-wind from the ERA-Interim reanalysis (supporting information Figure S4). The lack of robust trend in the MJO

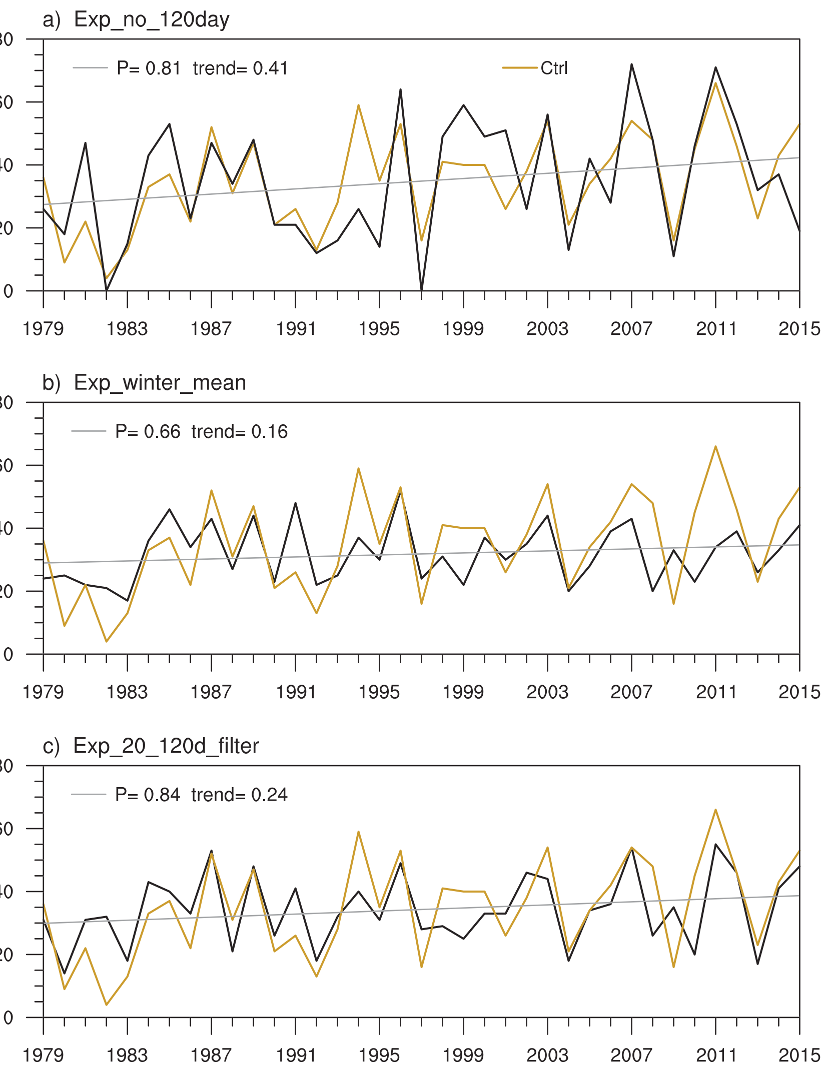

Figure 3. Days of the MJO Phases 4–6 during winters (November–April) from 1979 to 2015 based on different experiments: (a) Exp_no_120day experiment (black) along with CTRL (brown); (b) Exp_winter_mean experiment; (c) Exp_20_120d_filter experiment. Lines in each panel represent the linear trends in MJO Phase 4–6 days during the 36 winters in Exp_no_120day, Exp_winter_mean, and Exp_20_120d_filter, respectively, with the amplitude of the trend (units: days yr^{-1}) and significance *P* values labelled in corresponding legends.

Phase 4–6 days in Exp_winter_mean and Exp_20_120d_filter is also consistent with very similar MJO propagation characteristics during the two periods of 1979–1988 and 2006–2015 (supporting information Figure S5).

The weak positive trend in Exp_no_120day could be partially associated with the decadal regime shift in the tropical mean state characterized by strengthening of the Walker circulation and a grand La Niña pattern in late 1990s (e.g., Cai et al., 2019; Luo et al., 2012; Xiang & Wang, 2012; Yu et al., 2017), which is readily seen from the interannual variations in winter mean equatorial u-wind anomalies (Figure 4a). Projection of the enhanced convection near the MC and associated anomalous circulations onto the MJO will lead to more MJO Phase 4–6 days after late 1990s as clearly evident in Fig. 3a. Considering the stronger and robust positive trend in the MJO Phase 4–6 days in CTRL than that from Exp_no_120day, it suggests that this trend tends to be enhanced by removal of previous 120-day mean. This is further supported by Exp_120day_centered, where the 120-day mean is derived by the average over the 60 days before and 60 days after, instead of previous 120 days in CTRL. By doing so, the significant trend in MJO Phase 4–6 days as seen in CTRL is greatly weakened and becomes statistically insignificant in Exp_120day_centered (Figure S3a). Meanwhile, a

10.1029/2019GL086133

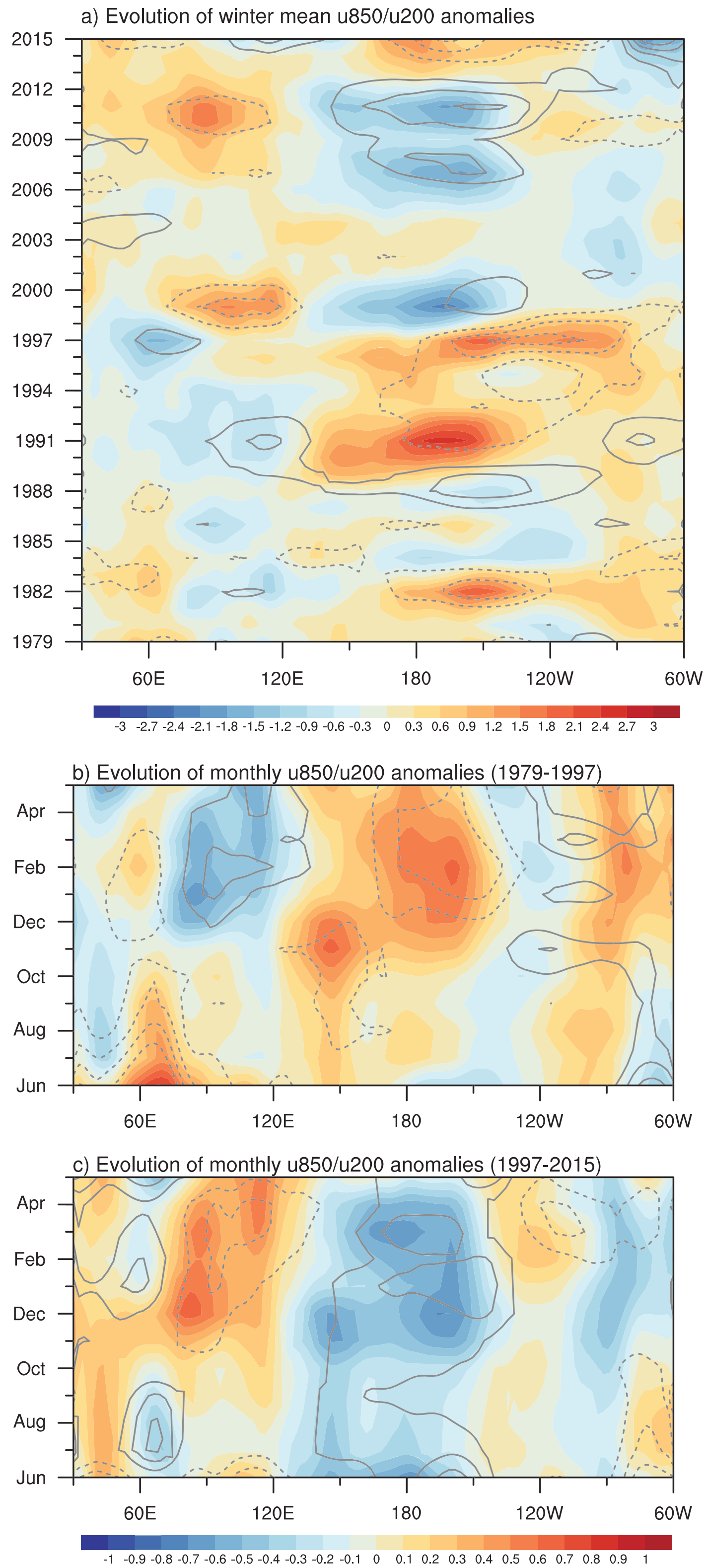

Figure 4. (a) Evolution of winter mean (November–April) u850 (shaded; see the color bar with units of m s^{-1}) and u200 (contour) anomalies for the period of 1979–2015; (b) Evolution of monthly mean u850 (shaded; see the color bar at the bottom with units of m s^{-1}) and u200 (contour) anomalies averaged over 1979–1997 and (c) 1997–2015. The contour intervals for u200 wind in (a) is 1.5 m s^{-1} with zero lines omitted and 0.4 m s^{-1} for (b) and (c). All fields are averaged over 15°S–15°N.

pronounced positive trend in the difference of MJO Phase 4–6 days between CTRL and Exp_120day_centered is clearly illustrated in Figure S3b, confirming that the removal of previous 120-day mean is largely responsible for the positive trend in MJO Phase 4–6 days in CTRL.

Further analyses suggest that the decadal change in anomalous circulation exhibits strong seasonal cycle. The maximum anomalous circulation associated with strengthening (weakening) of the Walker circulation after (before) late 1990s tends to occur during boreal winter season from November to April, with a seasonal transition from a summer regime around October (Figures 4b and 4c), which could be associated with meridional migration of the Asian monsoon system (Li et al., 2017). As a result, the observed trend in winter mean circulation tends to be effectively removed by subtracting the winter mean value or 120-day running mean centered on a particular winter day. When the previous 120-day mean is used to remove the winter anomalies in CTRL, however, the low-frequency winter circulation anomalies will not be effectively removed and even be amplified due to the involvement of summer circulation, which often shows an opposite sign over the Indian Ocean (Figures 4b and 4c), leading to a strong projection of more (less) MJO Phase 4–6 days after (before) 1997 in CTRL.

Summary

As a prominent intraseasonal variability mode of tropical atmosphere, the MJO plays a pivotal role in the global hydrological cycle. Improved understanding of changes in MJO activity and associated climate and weather extremes during the past decades, therefore, can provide important guidance for climate prediction and projection. It was recently reported that the frequency of convectively active MJO phases over the MC and WP, defined by the MJO Phase 4-6 days following WH04, is significantly increased in winters during the recent decades, which is further hypothesized to be critical in attributing to the recent Arctic warming through a so-call tropically excited Arctic warming mechanism.

However, this study suggests that the significant positive trend in the MJO Phase 4–6 days during the 36 winters could be exaggerated due to the blended signals of the low-frequency variability in the RMM MJO index. When deriving the RMMs in WH04, the OLR, u850, and u200 are subject to removal of their mean values over previous 120 days in addition to their climatological seasonal cycle, to exclude the low-frequency signals. Sensitivity experiments illustrate that the increasing trend in the MJO Phase 4–6 days during the past 36 winters is largely introduced by removal of the previous 120-day mean. When daily RMMs during each winter are reconstructed by calculating anomalies of the three variables by removing their winter mean instead of the previous 120-day mean, the robust increasing trend in the MJO Phase 4–6 days can no long be detected. The involvement of OLR and particularly circulation anomalies associated with the large-scale variability during summer/fall when calculating the winter RMM indices, which are included in the previous 120-day mean, is largely responsible for the overestimated trend by using the original RMM index.

This study, therefore, calls for cautions when employing the WH04 RMM index for studies of the low-frequency variability and climate trend in MJO activity and applications of the derived MJO variability for interpretation of changes in the climate systems. The impact of the inaccuracy in the derived real-time MJO status due to the projection from the low-frequency variability signals on MJO predictive skill also need to be assessed in future studies.

Acknowledgments
M. L. and Z. W. are jointly supported by the National Natural Science Foundation of China (grant 41790475) and the National Key Research and Development Program of China (grant 2016YFA0601801). X. J. acknowledges support by the NOAA Climate Program Office under awards NA15OAR4310098, NA15OAR4310177, and NA17OAR4310261. The RMM index can be accessed from the website (http://www.bom.gov.au/climate/mjo/). The NCEP-NCAR reanalysis data can be taken from the website (https://www.esrl.noaa.gov/psd/data/gridded/).

References

Adames, Á. F., Kim, D., Sobel, A. H., Del Genio, A., & Wu, J. (2017). Changes in the structure and propagation of the MJO with increasing CO_2. *Journal of Advances in Modeling Earth Systems*, *9*, 1251–1268. https://doi.org/10.1002/2017MS000913

Arnold, N. P., Branson, M., Kuang, Z., Randall, D. A., & Tziperman, E. (2015). MJO Intensification with warming in the superparameterized CESM. *Journal of Climate*, *28*, 2706–2724. https://doi.org/10.1175/jcli-d-14-00494.1

Baggett, C. F., Nardi, K. M., Childs, S. J., Zito, S. N., Barnes, E. A., & Maloney, E. D. (2018). Skillful subseasonal forecasts of weekly tornado and hail activity using the Madden-Julian Oscillation. *Journal of Geophysical Research-Atmospheres*, *123*, 12–661. https://doi.org/10.1029/2018JD029059 -612,675

Bui, H. X., and E. D. Maloney (2018), Changes in Madden-Julian Oscillation precipitation and wind variance under global warming, *45*, doi:https://doi.org/10.1029/2018GL078504, 7148-7155.

Cai, W., Wu, L., Lengaigne, M., Li, T., McGregor, S., Kug, J.-S., et al. (2019). Pantropical climate interactions. *Science*, *363*, 10.1126/science.aav4236, eaav4236.

Chang, C.-W. J., Tseng, W.-L., Hsu, H.-H., Keenlyside, N., & Tsuang, B.-J. (2015). The Madden-Julian Oscillation in a warmer world. *Geophysical Research Letters*, *42*, 6034–6042. https://doi.org/10.1002/2015GL065095

Duchon, C. E. (1979). Lanczos filtering in one and two dimensions. *Journal of Applied Meteorology*, *18*, 1016–1022.

Gottschalck, J., Wheeler, M., Weickmann, K., Vitart, F., Savage, N., Lin, H., et al. (2010). A framework for assessing operational Madden–Julian Oscillation forecasts: A CLIVAR MJO working group project. *Bulletin of the American Meteorological Society*, *91*, 1247–1258. https://doi.org/10.1175/2010BAMS2816.1

Hoskins, B. J., & Karoly, D. J. (1981). The steady linear response of a spherical atmosphere to thermal and orographic forcing. *Journal of the Atmospheric Sciences*, *38*, 1179–1196.

Jiang, X., Xiang, B., Zhao, M., Li, T., Lin, S.-J., Wang, Z., & Chen, J.-H. (2018). Intraseasonal tropical cyclogenesis prediction in a global coupled model system. *Journal of Climate*, *31*, 6209–6227. https://doi.org/10.1175/JCLI-D-17-0454.1

Jones, C., & Carvalho, L. M. V. (2006). Changes in the activity of the Madden-Julian Oscillation during 1958–2004. *Journal of Climate*, *19*, 6353–6370. https://doi.org/10.1175/JCLI3972.1

Jones, C., & Carvalho, L. M. V. (2011). Will global warming modify the activity of the Madden-Julian Oscillation? *Quart. J. Roy. Meteor. Soc.*, *137*, 544–552. https://doi.org/10.1002/qj.765

Kalnay, E., Kanamitsu, M., Kistler, R., Collins, W., Deaven, D., Gandin, L., et al. (1996). The NCEP/NCAR 40-year reanalysis project. *Bulletin of the American Meteorological Society*, *77*, 437–471.

Kiladis, G. N., Dias, J., Straub, K. H., Wheeler, M. C., Tulich, S. N., Kikuchi, K., et al. (2013). A comparison of OLR and circulation-based indices for tracking the MJO. *Monthly Weather Review*, *142*, 1697–1715. https://doi.org/10.1175/MWR-D-13-00301.1

Lau, W. K.-M., & Waliser, D. E. (2012). *Intraseasonal variability in the atmosphere-ocean climate system* (2nd ed., p. 613). Heidelberg, Germany: Springer.

Lee, C.-Y., Camargo, S. J., Vitart, F., Sobel, A. H., & Tippett, M. K. (2018). Sub-seasonal tropical cyclone genesis prediction and MJO in the S2S dataset. *Weather Forecasting*, *33*. https://doi.org/10.1175/waf-d-17-0165.1

Lee, S. (2014). A theory for polar amplification from a general circulation perspective. *Asia-Pacific Journal of Atmospheric Sciences*, *50*, 31–43. https://doi.org/10.1007/s13143-014-0024-7

Lee, S., Gong, T., Johnson, N., Feldstein, S. B., & Pollard, D. (2011). On the possible link between tropical convection and the Northern Hemisphere Arctic surface air temperature change between 1958 and 2001. *Journal of Climate*, *24*, 4350–4367. https://doi.org/10.1175/2011jcli4003.1

Lee, S.-H., & Seo, K.-H. (2011). A multi-scale analysis of the interdecadal change in the Madden-Julian Oscillation. *Atmosphere*, *21*.

Li, C., Luo, J.-J., & Li, S. (2017). Impacts of different types of ENSO on the Interannual Seesaw between the Somali and the maritime continent cross-equatorial flows. *Journal of Climate*, *30*, 2621–2638. https://doi.org/10.1175/jcli-d-16-0521.1

Liebmann, B., & Smith, C. A. (1996). Description of a complete (interpolated) outgoing longwave radiation dataset. *Bulletin of the American Meteorological Society*, *77*, 1275–1277.

Lin, H. (2018). Predicting the dominant patterns of subseasonal variability of wintertime surface air temperature in extratropical Northern Hemisphere. *Geophysical Research Letters*, *45*, 4381–4389. https://doi.org/10.1029/2018GL077509

Lin, H., Brunet, G., & Derome, J. (2008). Forecast skill of the Madden-Julian Oscillation in two Canadian atmospheric models. *Monthly Weather Review*, *136*, 4130–4149. https://doi.org/10.1175/2008mwr2459.1

Liu, P., Li, T., Wang, B., Zhang, M., Luo, J.-j., Masumoto, Y., et al. (2013). MJO change with A1B global warming estimated by the 40-km ECHAM5. *Climate Dynamics*, *41*, 1009–1023. https://doi.org/10.1007/s00382-012-1532-8

Luo, J.-J., Sasaki, W., & Masumoto, Y. (2012). Indian Ocean warming modulates Pacific climate change. *Proceedings of the National Academy of Sciences*, *109*, 18,701–18,706. https://doi.org/10.1073/pnas.1210239109

Madden, R. A., & Julian, P. R. (1971). Detection of a 40–50 day oscillation in zonal wind in tropical Pacific. *Journal of the Atmospheric Sciences*, *28*, 702.

Maloney, E. D., Adames, Á. F., & Bui, H. X. (2019). Madden-Julian Oscillation changes under anthropogenic warming. *Nature Climate Change*, *9*, 26–33. https://doi.org/10.1038/s41558-018-0331-6

Mundhenk, B. D., Barnes, E. A., Maloney, E. D., & Baggett, C. F. (2018). Skillful empirical subseasonal prediction of landfalling atmospheric river activity using the Madden-Julian oscillation and quasi-biennial oscillation. *npj Climate and Atmospheric Science*, *1*, 20177. https://doi.org/10.1038/s41612-017-0008-2

Seo, K.-H., Lee, H.-J., & Frierson, D. M. W. (2016). Unraveling the teleconnection mechanisms that induce wintertime temperature anomalies over the Northern Hemisphere continents in response to the MJO. *Journal of the Atmospheric Sciences*, *73*, 3557–3571. https://doi.org/10.1175/JAS-D-16-0036.1

Slingo, J. M., Rowell, D. P., Sperber, K. R., & Nortley, F. (1999). On the predictability of the interannual behaviour of the Madden-Julian Oscillation and its relationship with El Niño. *Quart. J. Roy. Meteor. Soc.*, *125*, 583–609. https://doi.org/10.1002/qj.49712555411

Song, E.-J., & Seo, K.-H. (2016). Past- and present-day Madden-Julian Oscillation in CNRM-CM5. *Geophysical Research Letters*, *43*, 4042–4048. https://doi.org/10.1002/2016GL068771

Stan, C., Straus, D. M., Frederiksen, J. S., Lin, H., Maloney, E. D., & Schumacher, C. (2017). Review of tropical-extratropical teleconnections on intraseasonal time scales. *Reviews of Geophysics*, *55*, 902–937. https://doi.org/10.1002/2016RG000538

Straub, K. H. (2013). MJO initiation in the real-time multivariate MJO index. *Journal of Climate*, *26*, 1130–1151. https://doi.org/10.1175/JCLI-D-12-00074.1

Vitart, F. (2017). Madden-Julian Oscillation prediction and teleconnections in the S2S database. *Quart. J. Roy. Meteor. Soc.*, *143*, 2210–2220. https://doi.org/10.1002/qj.3079

Vitart, F., Robertson, A., & Anderson, D. (2012). Sub-seasonal to seasonal prediction project: Bridging the gap between weather and climate. *WMO Bulletin*, *61*, 23–28.

Vitart, F., & Robertson, A. W. (2018). The sub-seasonal to seasonal prediction project (S2S) and the prediction of extreme events. *npj Climate and Atmospheric Science*, *1*, 3. https://doi.org/10.1038/s41612-018-0013-0

Waliser, D. E. (2012). *Predictability and forecasting, in Intraseasonal Variability in the Atmosphere-Ocean Climate System, edited by W. K. M. Lau and D. E.* Heidelberg, Germany: Waliser, Springer.

Wallace, J. M., & Gutzler, D. S. (1981). Teleconnections in the geopotential height field during the Northern Hemisphere winter. *Monthly Weather Review*, *109*, 784–812. https://doi.org/10.1175/1520-0493(1981)109<0784:TITGHF>2.0.CO;2

Wang, Z., Li, W., Peng, M. S., Jiang, X., McTaggart-Cowan, R., & Davis, C. A. (2018). Predictive skill and predictability of North Atlantic tropical cyclogenesis in different synoptic flow regimes. *Journal of the Atmospheric Sciences*, *75*, 361–378. https://doi.org/10.1175/jas-d-17-0094.1

Wheeler, M. C., & Hendon, H. H. (2004). An all-season real-time multivariate MJO index: Development of an index for monitoring and prediction. *Monthly Weather Review*, *132*, 1917–1932.

Wolding, B. O., Maloney, E. D., Henderson, S., & Branson, M. (2017). Climate change and the Madden-Julian oscillation: A vertically resolved weak temperature gradient analysis. *Journal of Advances in Modeling Earth Systems*. https://doi.org/10.1002/2016MS000843 n/a-n/a

Xiang, B., Lin, S.-J., Zhao, M., Johnson, N. C., Yang, X., & Jiang, X. (2019). Subseasonal week 3–5 surface air temperature prediction during boreal wintertime in a GFDL model. *Geophysical Research Letters*, *46*, 416–425. https://doi.org/10.1029/2018GL081314

Xiang, B., Lin, S.-J., Zhao, M., Zhang, S., Vecchi, G., Li, T., et al. (2015). Beyond weather time-scale prediction for hurricane sandy and super typhoon Haiyan in a global climate model. *Monthly Weather Review*, *143*, 524–535. https://doi.org/10.1175/MWR-D-14-00227.1

Xiang, B., & Wang, B. (2012). Mechanisms for the advanced Asian summer monsoon onset since the mid-to-late 1990s. *Journal of Climate*, *26*, 1993–2009. https://doi.org/10.1175/JCLI-D-12-00445.1

Xiu, J., Wen, M., Wang, Z., & Zhang, R. (2019). Interdecadal variation of the MJO propagation during the boreal winter in the context of global climate change. *Chinese Journal of Atmospheric Sciences (in Chinese with English abstract)*, *43*(1), 155–170. https://doi.org/10.3878/j.issn.1006-9895.1804.17278

Yoo, C., Feldstein, S., & Lee, S. (2011). The impact of the Madden-Julian Oscillation trend on the Arctic amplification of surface air temperature during the 1979–2008 boreal winter. *Geophysical Research Letters*, *38*, L24804. https://doi.org/10.1029/2011GL049881

Yoo, C., Lee, S., & Feldstein, S. B. (2012). Mechanisms of Arctic surface air temperature change in response to the Madden-Julian Oscillation. *Journal of Climate*, *25*, 5777–5790. https://doi.org/10.1175/JCLI-D-11-00566.1

Yu, J.-Y., Wang, X., Yang, S., Paek, H., & Chen, M. (2017). The changing El Niño-Southern Oscillation and associated climate extremes: Patterns and mechanisms. (pp. 1–38).

Zhang, C. (2013). Madden-Julian Oscillation: Bridging weather and climate. *Bulletin of the American Meteorological Society*, *94*, 1849–1870. https://doi.org/10.1175/bams-d-12-00026.1

Zhang, C. D. (2005). Madden-Julian Oscillation, *Reviews of Geophysics*., *43*, RG2003. https://doi.org/10.1029/2004RG000158